

Wound Healing-Promoting Effects of Apelin-13 in a CCD-1072Sk Fibroblast-Based In Vitro Model

Aykut Oruç^{1*} , Kadriye Yağmur Oruç² , Gökhan Ağtürk³ , Hakkı Oktay Seymen¹ 

¹ Department of Physiology, Cerrahpaşa Faculty of Medicine, Istanbul University-Cerrahpaşa, Istanbul, Türkiye

² Department of Physiology, Faculty of Medicine, Istinye University, Istanbul, Türkiye

³ Department of Physiology, Faculty of Medicine, Haliç University, Istanbul, Türkiye

Received: 2025-07-08

Accepted: 2025-09-18

Published Online: 2025-09-06

Corresponding Author

Aykut Oruç, MD

Address: Department of Physiology,
Cerrahpaşa Faculty of Medicine, Istanbul
University-Cerrahpaşa, Istanbul, Türkiye

E-mail: aykut.oruc@iuc.edu.tr

© 2025. The copyright of this article is retained by the author(s).

OPEN  ACCESS



This work is licensed under a [Creative Commons Attribution-NonCommercial 4.0 International License](https://creativecommons.org/licenses/by-nc/4.0/).

This license permits the free sharing and adaptation of the work for non-commercial purposes, provided that appropriate attribution is given to the original author(s) and to its initial publication in this journal.

ABSTRACT

Objective: As an intricate process, wound healing involves contributions from numerous cell types. Fibroblasts critically support wound healing via sustaining the integrity of the extracellular matrix, promoting collagen synthesis, and driving contraction during proliferation and remodeling. A balanced inflammatory response is essential for this repair. The apelinergic system, comprising Apelin and APJ (apelin receptor)—abundantly found in the skin and scar fibroblasts—plays a significant regulatory role. This is among the first to reveal the role of exogenous Apelin-13 in wound healing using a scratch model in CCD-1072Sk fibroblast cell line.

Methods: The doses of 2 and 5- $\mu\text{g/ml}$ Apelin-13 were chosen based on the cell viability assay result. After seeding cells in 24-well plates, the wound scratch model was applied once they reached approximately 90% confluency. Samples of the control (CTL), A-2, and A-5 groups were collected and analyzed at 0 h (hour) (baseline), 24 h, 48 h, and 72 h. After the wound scratch model, the wound gap area was checked at the relevant time points. ELISA analysis was performed for levels of TGF- β 1, TNF- α , and IL-10. Apoptosis was analyzed with a fluorescent microscope using the Annexin V-FITC/PI method.

Results: In the viability assay, 2 and 5 $\mu\text{g/ml}$ Apelin-13 doses were used. Wound closure decreased significantly at all time points in both Apelin groups vs. 0 h ($p < 0.001$). Apoptosis increased significantly in A-2-48 and A-5-48 groups ($p < 0.001$). TNF- α decreased in A-2 vs. CTL ($p < 0.001$) and A-5-72 ($p < 0.001$). TGF- β 1 increased in A-5-72 vs. A-2-72 ($p < 0.05$). IL-10 increased in all Apelin groups vs. CTL ($p < 0.001$).

Conclusion: Apelin-13 promoted wound healing by balancing inflammation, enhancing fibroblast proliferation, migration, and reducing apoptosis. 2 $\mu\text{g/ml}$ Apelin-13 showed notable effects, while 5 $\mu\text{g/ml}$ was superior at certain time points. Apelin-13 appears to be a promising wound-healing agent.

Keywords: Apelin-13, CCD-1072Sk, fibroblast, fibrosis, scratch assay, wound healing

INTRODUCTION

Wound healing is a highly orchestrated mechanism in which many molecular events take place for the effective repair of damaged tissue and for it to regain its former physiological functions and integrity [1]. This dynamic phenomenon is carried out by the coordinated and synergistic work of signals from various cells, growth factors, and biochemical molecules [2]. In pathologies where healing is impaired, such as diabetic ulcers [3], chronic venous-arterial wounds [4], and pressure ulcers [5], the risk of infection is high and causes a decrease in the quality of life with consequences ranging from sepsis to limb loss [6]. In vitro wound scratch assay is gaining importance in the analysis of migration, proliferation, wound gap closure mechanisms at the cellular level, and in observing drug-biomolecule testing, as it provides repetitive and controlled results [7].

Fibroblasts are pivotal in fundamental cascades of wound healing, including fibrinolysis, wound contraction, rebuilding of extracellular matrix (ECM), and collagen structures [8-11]. In the inflammatory phase of wound healing, fibroblast cells produce tumor necrosis factor- α (TNF- α), a proinflammatory cytokine [12]. Interleukin-10 (IL-10), produced by fibroblasts, promotes granulation tissue formation during the proliferation phase and prevents excessive proinflammatory mediator release [13]. During the remodeling phase, IL-10 promotes collagen fiber restructuring and enhances scar tissue stabilization [13, 14]. Tumor Growth Factor- β (TGF- β) is secreted by cells such as fibroblasts, epithelial, and immune cells and functions in most phases of wound healing [15, 16].

The apelin peptide ligand and the G-protein-coupled apelin receptor (APJ) together constitute the apelinergic system [17]. Apelin is initially synthesized in adipose tissue as a 77-amino acid pre-proapelin and is then cleaved by peptidases to convert

into various endogenous bioactive isoforms, including apelin-13, 12, 17, 36, 55 [18]. Endogenous apelin has been reported to be involved in angiogenesis during ischemia, and exogenous apelin administration is involved in wound healing [19-21]. The apelinergic system has been reported to be expressed in a broad spectrum in scar tissue fibroblasts and normal skin fibroblasts [22].

Based on this information, the objective of this study is to investigate the role of fibroblasts in the wound healing process by creating a scratch wound model in the CCD-1072Sk normal skin fibroblast cell line and the effect of the apelin/APJ signaling pathway on this process with exogenous apelin-13 treatment.

MATERIALS AND METHODS

Cell Culture

Experiments were performed in Haliç University Faculty of Medicine and Istanbul University-Cerrahpaşa, Cerrahpaşa Faculty of Medicine, Physiology Research Laboratories. The CCD-1072Sk Human Skin Fibroblast Cell Line used in our experiments was obtained from the American Type Culture Collection (CCD-1072Sk (ATCC-CRL-2088); USA) by passage six and cultured in a sterile laminar flow. Cells from the liquid nitrogen tank at -196 °C were gradually thawed and transferred to 25 cm² flasks. Cells were cultured in Dulbecco's Modified Eagle Medium Nutrient Mixture F-12 (DMEM-F12, Gibco, Thermo Fisher) supplemented with 1% antibiotic (Penicillin/Streptomycin, Gibco, Thermo Fisher) and incubated at 37 °C with 5% CO₂ in an incubator (CO₂ Incubator, MCO-170AC-PE, PHC Corporation, Japan). After incubation, CCD-1072Sk cells were checked with an inverted (PrimoVert-Inverted Microscope-Carl Zeiss Microscopy) microscope, and trypsinization was carried out with Trypsin-EDTA (Gibco, Thermo Fisher) once cells reached 80-90% confluency.

Cell Passaging

During the passaging process, the medium was aspirated, and debris was removed by PBS washing. Trypsin-EDTA (0.25%) was added and incubated for 3 minutes at 37 °C with 5% CO₂. Cells were taken into sterile tubes and centrifuged at 1300 rpm; the supernatant was discarded, and medium was added to the pellet. Cells placed in T75 flasks were incubated at 37 °C with 5% CO₂.

Cell Viability Test (MTT Assay)

The 3-(4,5-dimethylthiazol-2-yl)-2,5 diphenyltetrazolium bromide (Cell Proliferation Kit I (MTT) 11465007001, Roche)

Main Points

- Apelin-13 enhances wound healing by modulating inflammation and promoting fibroblast migration, proliferation, and survival.
- The 2 µg/ml dose showed significant effects, while 5 µg/ml was more effective at certain stages, suggesting a stage-specific dosing strategy.
- Sequential high-to-low dosing of Apelin-13 aligned with wound healing phases may optimize therapeutic outcomes, warranting further research.

assay was conducted on CCD-1072Sk cell line at 24, 48, and 72 hours. For the evaluation of cytotoxic responses in Apelin-13 (Cayman Chemicals, 13523, USA) treated groups, cells were distributed into 96-well plates at a seeding density of 1×10^5 . Apelin-13 was applied at doses of 1, 2, 5, 10 $\mu\text{g/ml}$. Formazan crystals were quantified according to the kit manual. 2 and 5 $\mu\text{g/ml}$ Apelin-13 doses were selected. Three experimental groups were formed: Control, A-2, and A-5.

Wound Scratch Assay

5×10^4 cells were cultured in 24-well plates, and after verifying that the cells reached 90% confluency with an inverted microscope, in the center of each well was marked with a scratch with a 300 μL pipette tip. Then, the wound line was checked under an inverted microscope for 0, 24, 48, and 72 hours, with 10x-40x magnification applied and photographs were taken with the integrated camera. The area of wound closure was measured with ImageJ.

Enzyme-Linked Immunosorbent Assay (ELISA) Analyses

Anti-inflammatory cytokines IL-10, TGF- β 1, and the proinflammatory cytokine TNF- α were measured in the supernatants of CCD-1072Sk cells via ELISA kits following the kit manual (Interleukin-10 IL-10 Cat. No. E0102Hu, tumor necrosis factor-alpha TNF- α Cat. No. E0082Hu, transforming growth factor-beta TGF- β 1 Cat. No. E0134Hu; BT LAB, Shanghai, China).

Apoptosis Staining

Annexin-V-FITC/PI Apoptosis Kit was obtained from the manufacturer (Elabscience Bionovation Inc., Annexin V-FITC/PI Apoptosis Kit, Cat. No: E-CK-A211, Texas, US). Annexin V is a high-affinity binding protein for Ca^{2+} -dependent phosphatidylserine. Annexin V is used with propidium iodide (PI), which can bind to nucleic acids, allowing apoptotic staining [23]. CCD-1072Sk cells cultured in a 24-well plate, seeding density of 1×10^5 cells/well. The manufacturer's instructions were followed when performing the apoptosis analysis.

For the quantitative evaluation of Annexin V-PI fluorescence staining, five fields were randomly selected in 3 replicate wells for each group and 300-350 CCD-1072Sk cells photographed using 10x-40x magnifications using an inverted fluorescence microscope (Carl Zeiss TM, Axio Vert.A1 FL-LED Inverted Microscope, Germany) and software (Carl Zeiss, AxioCam 506, ZEN 2 Lite Software, Germany). Automatic cell counts were

performed using ImageJ (ImageJ, NIH, United States) and were also confirmed by manual counting. Apoptosis photographs are representative of five randomly selected fields per group under 40x magnification [24, 25].

Statistical Analyses

All statistical analyses were conducted with the GraphPad Prism program (Version 10.2.0, United States). The normality was tested using the Shapiro-Wilk test, and homogeneity was tested using the Levene Test. Data were normally distributed and homogeneous. Comparisons across groups were analyzed with one-way ANOVA and Bonferroni post hoc correction. Wound healing gap closure percentage and Annexin-V-FITC/PI apoptosis were analyzed through repeated measures ANOVA and subsequent Bonferroni correction. All results are shown as mean \pm SD (standard deviation), considering $p < 0.05$ as statistically significant.

RESULTS

Cell Viability Assay

In the MTT viability analysis, no statistically significant difference was observed between the groups at hours 24 and 72. However, at hour 48, a decrease in cell count in the CCD-1072Sk fibroblast cell line was noted in A-10-48 compared to CTL-48 ($p < 0.01$). 1 $\mu\text{g/ml}$ Apelin-13 showed a weak protective effect, while 10 $\mu\text{g/ml}$ caused cytotoxicity. Therefore, 2 $\mu\text{g/ml}$ and 5 $\mu\text{g/ml}$ Apelin-13 doses were selected. The results of the Cell Viability analysis are summarized in the related figure and table (Figure 1, Table 1).

Wound Healing Gap Closure Percentage

When the wound healing closure percentages of Apelin-13 were considered, compared to the CTL-0 group, a decrease ($p < 0.001$) was observed in the CTL-24, CTL-48, and CTL-72. Compared to the A-2-0, a decrease ($p < 0.001$) was found in the A-2-72. Compared to the A-5-0, decrease ($p < 0.001$) was found in the A-5-72 group (Figure 2).

Compared to the CTL, it was observed that A-2 and A-5 Apelin-13 doses increased cell migration and wound closure rate. In the 0th hour images, the baseline was similar in all groups. At 24h, it was observed that cell migration was faster in the A-2 and A-5 compared to the CTL. At 48h, the closure rate of cells was higher compared to the CTL, especially in the A-2. At 72h, it was determined that the wound area closed more in the A-2 and A-5 compared to the CTL (Figure 3).

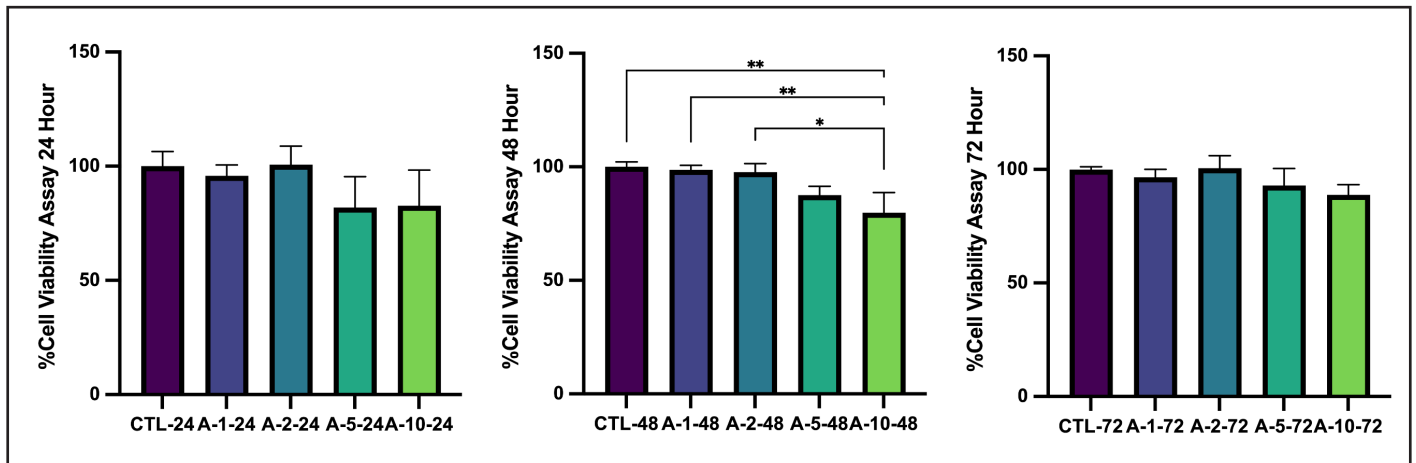


Figure 1. Statistical graphs of viability assay (MTT) in CCD-1072Sk fibroblast cell line. Cell Viability results of Apelin-13 on the CCD-1072Sk fibroblast cell line at 24th hour (A), 48th hour (B), 72th hour (C). Data were normalized to the control groups. CTL: control group; A-2: Apelin-13 group (2 μg/ml); A-5: Apelin-13 group (5 μg/ml). Each condition was tested triplicate. Statistical analysis was performed using one-way ANOVA with Bonferroni post-hoc correction and data are presented as mean ± SD (GraphPad Prism software). Statistical significance: $p < 0.05$ (*), $p < 0.01$ (**), $p < 0.001$ (***)

Table 1. Viability Assay Values (Mean ± SD)

Viability Assay 24h	CTL-24	A-1-24	A-2-24	A-5-24	A-10-24
Mean ± SD	100.0 ± 6.4	95.85 ± 4.7	100.7 ± 8.1	81.99 ± 13.4	82.71 ± 15.6
48h	CTL-48	A-1-48	A-2-48	A-5-48	A-10-48
Mean ± SD	100.0 ± 2.1	98.68 ± 2.02	97.64 ± 3.8	87.55 ± 3.8	79.79 ± 8.9
72h	CTL-72	A-1-72	A-2-72	A-5-72	A-10-72
Mean ± SD	100.0 ± 1.3	96.60 ± 3.5	100.5 ± 5.6	92.93 ± 7.6	88.83 ± 4.5

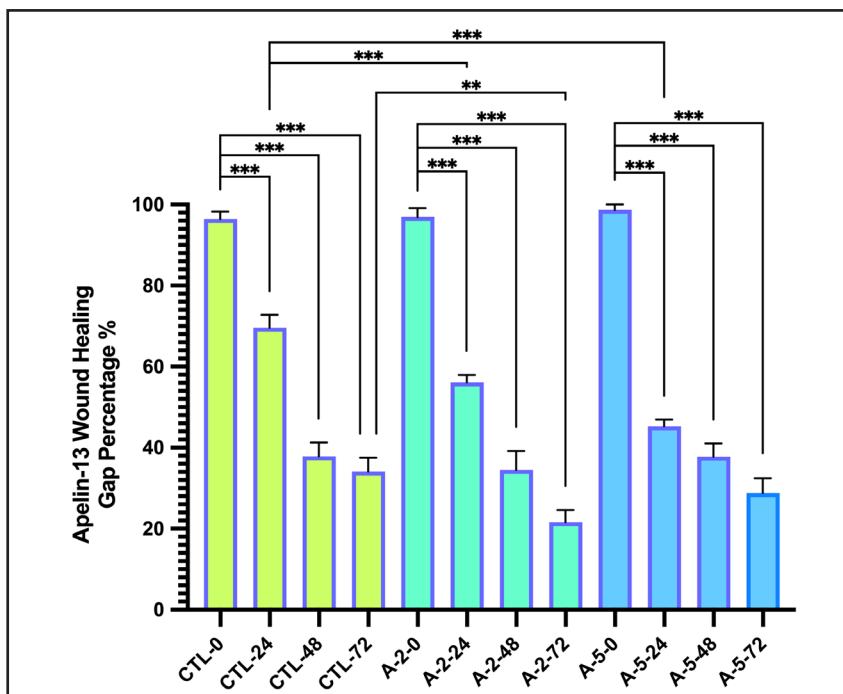


Figure 2. Quantitative analysis of Apelin-13 on wound healing gap closure percentage at 0, 24, 48, 72 hours in CCD-1072Sk fibroblast cell line. Data were normalized to the control groups. CTL: control group; A-2: Apelin-13 group (2 μg/ml); A-5: Apelin-13 group (5 μg/ml). Each condition was tested triplicate. Statistical analysis was performed using one-way ANOVA with Bonferroni post-hoc correction and data are presented as mean ± SD (GraphPad Prism software). Statistical significance: $p < 0.05$ (*), $p < 0.01$ (**), $p < 0.001$ (***)

Apoptosis Analysis

Apoptosis % Cell Count

In the Apoptosis % Cell Count analysis, apoptosis rate compared to CTL-24 increased in A-2-24 ($p<0.001$), decreased in A-2-24 ($p<0.05$). Compared to CTL-48, increased in A-2-48 and A-5-48 ($p<0.001$). Compared to CTL-72 decreased in A-2-72 ($p<0.05$) and A-5-72 ($p<0.001$). A decrease ($p<0.001$) observed in A-2-24 compared to A-5-24. A-2-48 group compared to the A-2-24, A-2-72, and A-5-48 compared to A-5-24, A-5-72 group showed higher apoptosis rate ($p<0.001$) (Figure 4).

Annexin-V-FITC/PI Apoptosis staining

In the Annexin-V-FITC/PI Apoptosis staining the highest apoptosis rate was observed in the A-2-48. An increase was observed in A-2-24 Annexin V(+) early apoptotic cells compared to CTL-24. In the A-5-24, although the rate of Annexin V(+) early apoptotic cells was higher compared to A-2-24, the number of PI(+) dead/necrotic cells was low compared to the CTL and A-2-24. In the A-2-48, an increase in the number of Annexin V(+) early apoptotic cells compared to A-5-48. Number of Annexin V(+) early apoptotic cells quite low in the A-2-72 and A-5-72 compared to 24., 48. hour groups. In merged images, it is especially noticeable that the late apoptosis rate decreased significantly in the A-5-24, A-5-48, A-5-72 groups (Figure 5).

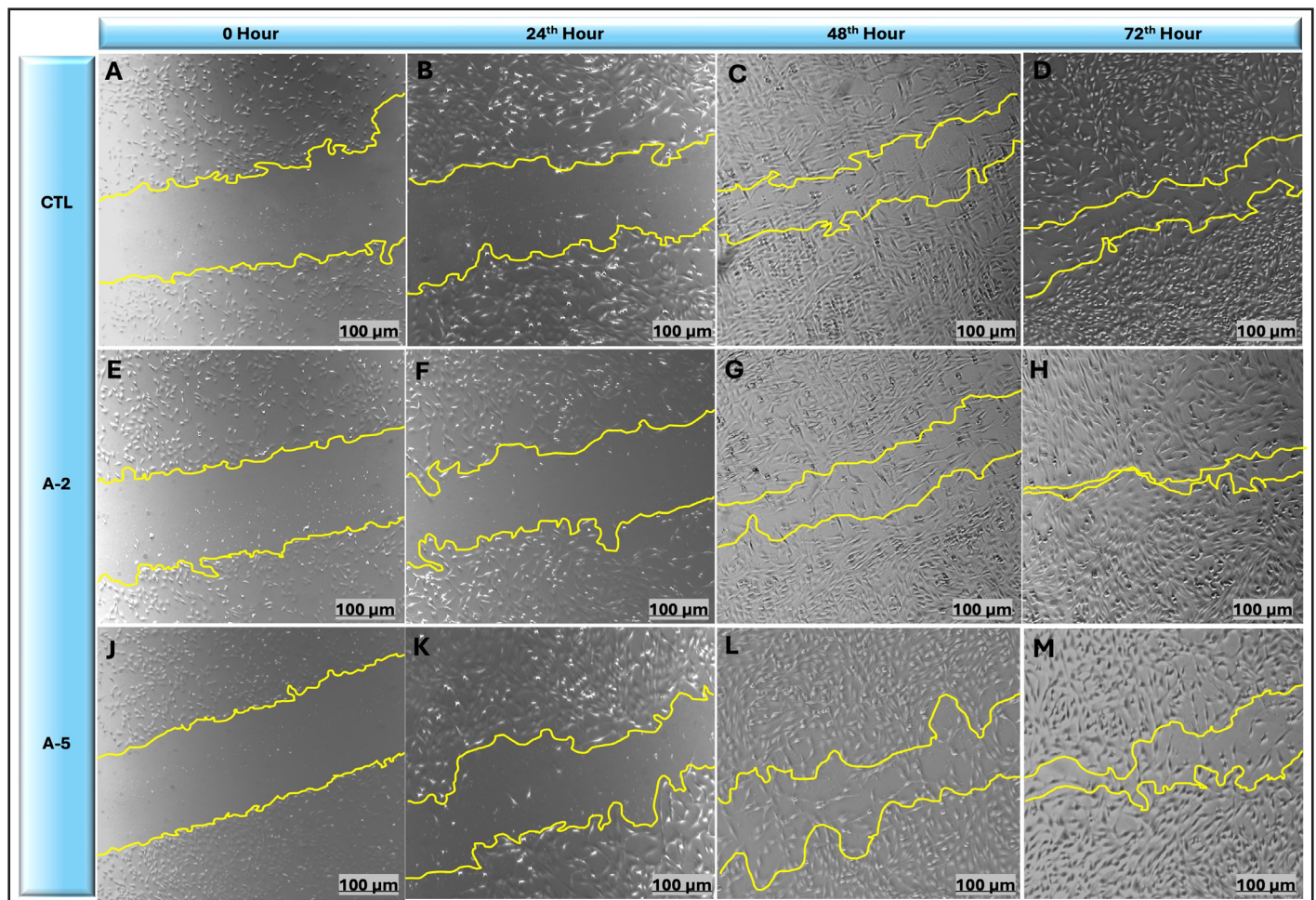


Figure 3. Images of the scratch wound assay in the CCD-1072Sk fibroblast cell line in CTL, A-2, and A-5 groups at 0, 24, 48, and 72 hours. CTL: control group; A-2: Apelin-13 group (2 µg/ml); A-5: Apelin-13 group (5 µg/ml). Yellow lines indicate cell migration and wound line closure during wound healing. Wound line edges were automatically delineated with the Straight-Line Tool using the yellow line. Wound surface area was measured using the Analyze Particles command. Measurements were performed using ImageJ software. The raw images were assembled in PowerPoint to create a publication-ready format and enriched by adding group and time bars. Wound gap closure line, CTL group at 0 hour (A), 24th (B), 48th (C), 72th hours (D), 2 µg Apelin-13 group at 0 (E), 24th (F), 48th (G), 72th hours (H) and 5 µg Apelin-13 group at 0 (J), 24th (K), 48th (L), 72th hours (M). Scale bars are 100 µm (10x magnification).

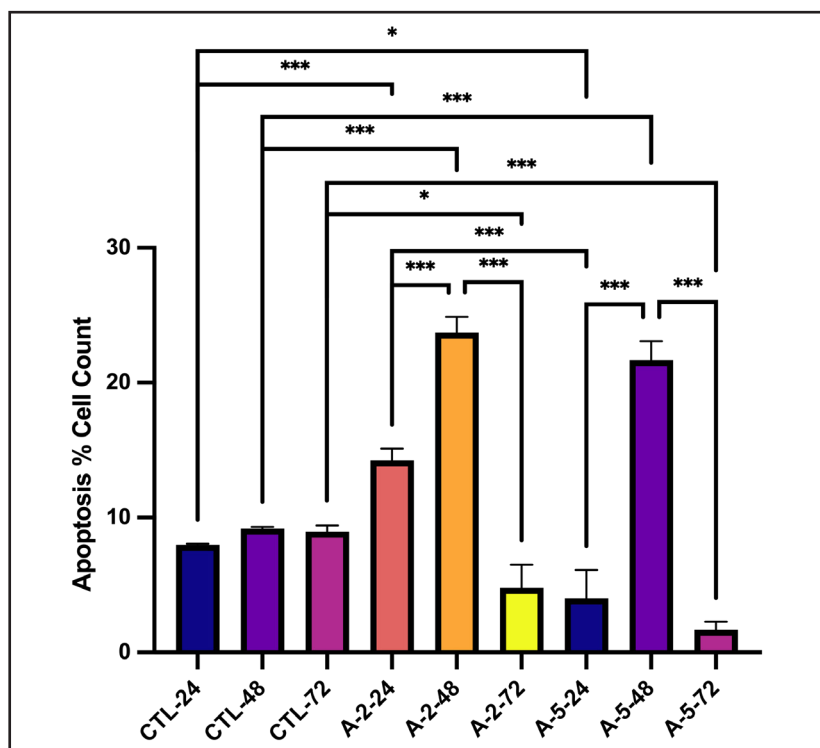


Figure 4. Apoptosis % Cell Count on CCD-1072Sk Fibroblast cell line. Data were normalized to the control groups. CTL: control group; A-2: Apelin-13 group (2 $\mu\text{g/ml}$); A-5: Apelin-13 group (5 $\mu\text{g/ml}$). Each condition was tested triplicate. Statistical analysis was performed using one-way ANOVA with Bonferroni post-hoc correction and data are presented as mean \pm SD (GraphPad Prism software). Statistical significance: $p < 0.05$ (*), $p < 0.01$ (**), $p < 0.001$ (***).

Enzym-Linked ImmunoSorbent Assay Analysis

TNF- α levels showed a gradual decrease at 24, 48, 72 hours in A-2 dose compared to CTL groups ($p < 0.001$), while A-5 groups showed an increase at the same time points compared to A-2 groups ($p < 0.001$) and no significance was found in A-5 groups compared to CTL.

TGF- β 1 levels were increased in A-5-72 compared to CTL-72 ($p < 0.01$). IL-10 levels were increased in all A-2 groups compared to CTL groups at the same time point ($p < 0.001$), while A-5 groups were decreased compared to A-2 groups ($p < 0.001$). Furthermore, all A-5 groups were increased compared to CTL ($p < 0.001$). The results of ELISA analysis are summarized in the table (Figure 6, Table 2).

DISCUSSION

This study is the first to show that Apelin-13 supports wound healing in the CCD-1072Sk Human fibroblast cell line by suppressing the proinflammatory response and increasing the anti-inflammatory response, cell migration, and proliferation in a dose and time-dependent manner.

Wound healing is developed under the management of different molecules and cells, consisting of inflammation, proliferation, and remodeling phases [26]. The MTT test is the gold standard for evaluating drug toxicity [27].

Apelin-13 at doses of 0.01 μM , 0.1 μM , 1 μM , and 10 μM was reported to have no significant cytotoxicity in PC-12 pheochromocytoma cells according to MTT results at 24h, and 1 μM Apelin-13 dose significantly increased viability [28]. Apelin-13 doses of 1, 2.5, 5 and 10 $\mu\text{g/ml}$ were tested in the MTT test on the SH-SY5Y cell line and it was shown that the doses of 2.5 and 5 $\mu\text{g/ml}$ were not toxic and provided antioxidative protection [29]. In our study, 10 $\mu\text{g/ml}$ Apelin-13 was eliminated due to its cytotoxicity. Apelin-13 dose of 2 $\mu\text{g/ml}$ ($\approx 1.33 \mu\text{M}$) showed cell viability equivalent to the control group at 24, 48, and 72h. The fact that a 5 $\mu\text{g/ml}$ ($\approx 3.33 \mu\text{M}$) Apelin-13 dose temporarily decreased fibroblast viability at 24h, then gradually increased proliferative activity at 48h and 72h, approaching the CTL, indicates that the relevant dose only has a reversible cytostatic effect and transient cellular stress. These results support that we obtained results consistent with the literature in terms of dose.

One of the most important methods used to demonstrate cell migration and proliferation is the scratch wound healing test [30]. Wound healing consists of four basic phases: hemostasis, inflammation, proliferation, and remodelling [31]. The hemostasis phase is completed within the first hour, primarily mediated by thrombocytes, while the inflammation phase begins between 1-10 hours with the accompaniment of neutrophils, circulating and resident macrophages, and fibroblasts.

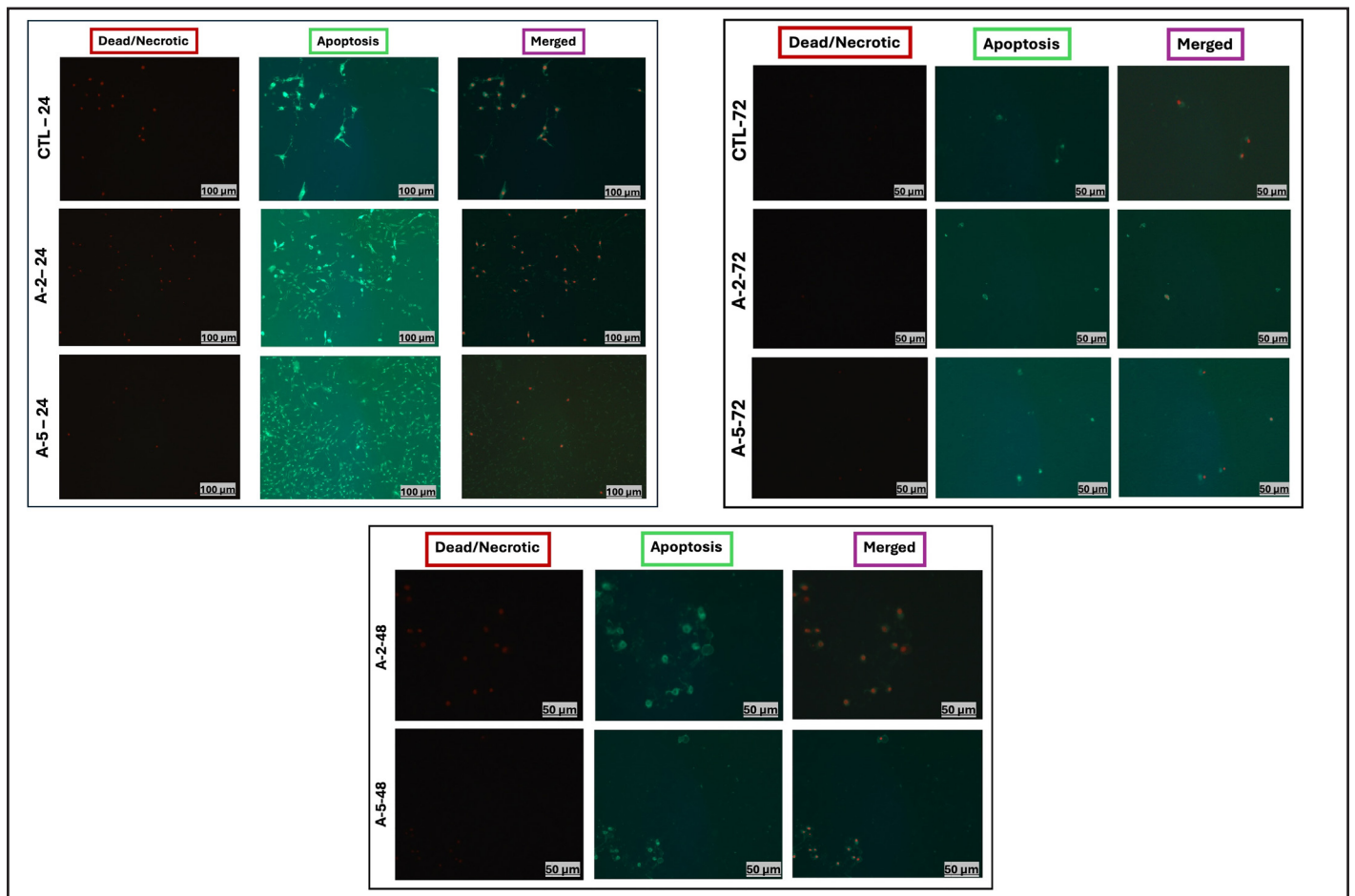


Figure 5. Representative fluorescence microscopy images showing apoptotic and necrotic cell populations in CTL and A-2, A-5 groups at 24, 48, 72 hours by Annexin-V-FITC/PI Apoptosis staining in the CCD-1072Sk fibroblast cell line. Green fluorescence indicates Annexin V-FITC positive (+) cells (early apoptosis), red fluorescence indicates PI positive (+) cells (dead/necrotic), and merge panels indicate late apoptotic cells. Control group at 24th hour (A), 48th hour (B), 72nd (C) hour. CTL: control group; A-2: Apelin-13 group (2 μg/ml); A-5: Apelin-13 group (5 μg/ml). Scale bars represent 100 μm (10x magnification) for 24 h images and 50 μm (40x magnification) for 48 and 72 h images. Images are representative of three independent experiments.

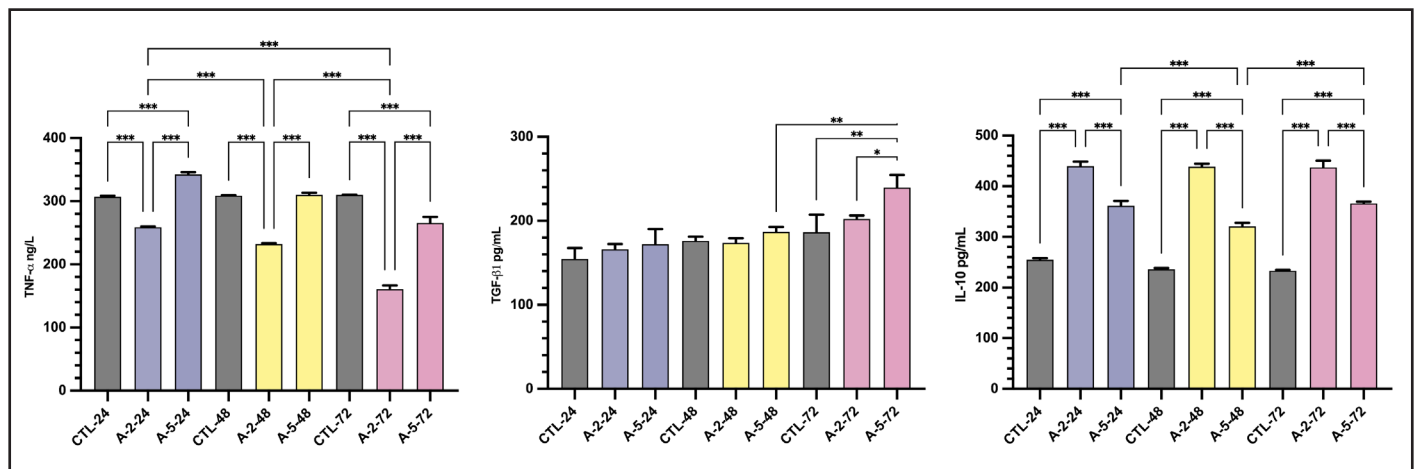


Figure 6. Statistical graphs of ELISA analysis performed on the CCD-1072Sk fibroblast cell line. TNF-α (A), TGF-β1 (B), IL-10 (C) ELISA analysis values in CTL, A-2 and A-5 groups at 24th, 48th and 72nd hours. Data were normalized to the control groups.

CTL: control group; A-2: Apelin-13 group (2 µg/ml); A-5: Apelin-13 group (5 µg/ml). Each condition was tested triplicate. Statistical analysis was performed using one-way ANOVA with Bonferroni post-hoc correction and data are presented as mean ± SD (GraphPad Prism software). Statistical significance: $p < 0.05$ (*), $p < 0.01$ (**), $p < 0.001$ (***)

Table 2. TNF- α (A), TGF- β 1 (B), IL-10 (C) ELISA analysis values in CTL, A-2 and A-5 groups at 24th, 48th and 72nd hours (Mean ± SD).

ELISA	CTL-24	A-2-24	A-5-24	CTL-48	A-2-48	A-5-48	CTL-72	A-2-72	A-5-72
TNF- α	306.9 ± 1.6	258.9 ± 1.3	342.6 ± 3.2	308.9 ± 0.5	232.2 ± 1.2	310 ± 3.5	309.9 ± 0.7	160.7 ± 6.1	265.4 ± 9.8
TGF- β 1	154.7 ± 13	166.1 ± 6.2	172.1 ± 17.9	176 ± 5.1	173.7 ± 5.5	186.9 ± 5.9	186.3 ± 21.2	202.2 ± 4.1	239.6 ± 15.1
IL-10	254.7 ± 3.4	439.7 ± 8.8	361.5 ± 9.4	236 ± 2.3	438.7 ± 5.7	320.8 ± 6.8	233 ± 1.8	437.2 ± 13.2	366 ± 3.4

Following the proliferation phase led by fibroblasts, which can last from 10 hours to 1 month, the matrix formation and remodelling phase continues from 72 hours to 1 year, and the wound eventually closes in about a year. These four stages also include sub-stages such as polymorphonuclear cell influx, M1-M2 macrophage class switch, re-epithelialization-granulation tissue formation (fibroblast proliferation), collagen deposition, angiogenesis, wound contraction, and maturation, which occur interdependently. Depending on the type of wound formation, the processes may be extended or shortened [11]. In this context, the time points we used as the basis in our study were modeled to symbolize the hemostasis process at the time of the damage at 0th hour, the inflammatory phase at 24th hour, the early phase of the proliferation phase at 48th hour, and the late phase of the proliferation phase and the remodeling phase at 72nd hour. In the wound model, exogenous pyr-apelin-13 suppresses pressure ulcer formation by inhibiting angiogenesis and oxidative stress [21]. Apelin has been reported to play a protective role in myocardial infarction by increasing vascular endothelial growth factor-2 expression, reducing cardiac microvascular endothelial cell permeability, and promoting angiogenesis [32]. Controlled release of Apelin-13 from thermosensitive biocompatible hydrogel decreased oxidative stress markers, increased anti-inflammatory response, and angiogenesis in skin flap treatment [33]. Apelin has also been reported to increase fibroblast cell migration [34]. In our study, the significant decrease in the wound gap percentage and increased migration in fibroblast cells at 0, 24, 48, and 72h with a dose of 2-µg Apelin-13 compared to the control indicates that Apelin-13 supports healing and migration. A dose of 5-µg Apelin-13 provided more effective wound closure at 24h compared to the control and 2-µg Apelin-13 doses. It is seen that the 2-µg Apelin-13 played a primary role

at 48-72h. This suggests that, depending on the dose and time, high-dose Apelin-13 treatment is effective in the early stages of wound healing in the first 24h, while low-dose Apelin treatment provides more effective healing and wound closure at 48-72h. This indicates that wound treatment can be started with high-dose Apelin and switched to low-dose.

APJs expressed in normal skin fibroblasts and scar tissue regulate the secretion of ECM proteins by fibroblasts. The apelin/APJ complex has been suggested as a new target for the treatment of scar tissue prevention [22]. TGF- β 1-induced fibrosis in systemic sclerosis patients was suppressed by apelin/APJ signaling [35].

Apoptosis is essential for the clearance of cells involved in inflammation in the early phase of wound healing and controlling scar formation [36]. Apelin-13/APJ signaling has been reported to suppress apoptosis [37-40]. In our study, the gradual increase in apoptosis in the A-2-24 group, which corresponds to the inflammatory phase following the normal wound healing process. The lower apoptotic rate observed in the A-5-24 group compared to CTL suggested that high-dose Apelin-13 may suppress inflammation more rapidly in the first 24 hours. At the 48h, which indicates the early phase of proliferation, compared to the CTL, suggested that there was a controlled elimination of active fibroblasts that had completed their task. The fact that apoptosis fell below control levels at 72h in both dose groups suggested that apoptotic signals decreased due to the successful and balanced completion of wound healing. In line with this information, the increased apoptosis in A-2 and A-5 groups (except A-5-24) and then a significant decreasing at the 72h, showed that apoptosis was carried out in a controlled manner within the context of physiological wound healing. This biphasic

pattern may be due to dose- and time-dependent modulation of apelin-13 for apoptosis. It may reflect the early survival signals, subsequent cellular stress, and adaptation.

TNF- α is a proinflammatory cytokine with multifactorial effects on cells [41]. In the early stages of cutaneous wound healing, TNF- α facilitates fibroblast and keratinocyte proliferation and immune cell mobilization, contributing to wound healing. However, excessively high levels can lead to scar tissue formation in persistent inflammation, which delays and impairs the wound healing process [42]. It has been reported in the literature that the use of anti-TNF- α monoclonal antibodies reduces the number of inflammatory cells and fibroblasts, delays wound closure, and accelerates wound healing with subsequent application of exogenous TNF- α treatment [43]. In our study, the increase in TNF- α in the 5- μ g Apelin-13 at 24h compared to the CTL shows that the high dose of Apelin-13 can be a trigger in the inflammatory context, but the speed of wound closure can be increased at this stage.

Fibroblasts secrete TGF- β and fibroblast growth factor along with the formation of the granulation tissue, thus providing wound contraction [44]. Subtype TGF- β 1 has important functions such as cellular growth and wound regeneration [45]. In the proliferative phase, re-epithelialization, angiogenesis, and fibroplasia occur. During fibroplasia, ECM components are produced by fibroblast migration, proliferation, and granulation tissue formation in the wound area. Migration of fibroblasts in the proliferation phase occurs via TGF- β 1 [16]. TGF- β 1 levels increase after the onset of epithelialization in the final stage of wound healing. Studies have shown that the use of TGF- β 1 antibodies in wound treatment can mimic intact skin [46]. TGF- β promotes wound contraction, increases ECM production, and promotes fibroblast differentiation [47]. Our study results, similar to the literature, show that low and high doses of Apelin-13 reduce the risk of fibrosis by increasing TGF- β 1 production in a controlled manner in the late phase of wound healing and increase fibroblast migration in the wound gap closure percentage.

IL-10 is an important anti-inflammatory cytokine in preventing scar tissue formation during wound healing and is expressed and secreted by granulocytes, keratinocytes, fibroblasts, endothelial cells, and mast cells [13, 44]. It regulates the type and number of immune cells that migrate to the injury site in the primary phase and the levels of proinflammatory cytokines,

facilitating the transition from the inflammatory phase to the proliferative phase. IL-10 is also protective against scar tissue formation in processes such as pulmonary fibrosis and myocardial infarction by reducing collagen production. In addition, proteolytic enzymes lyse the ECM through IL-10, and TGF- β 1 expression is reduced to prevent fibrosis [44]. IL-10 suppresses the inflammatory response and inhibits proliferation and collagen synthesis [48]. In our study findings, parallel to the literature, it was observed that IL-10 levels increased stably in all inflammation, proliferation, and remodeling stages in low and high dose Apelin-13 applications compared to the control. However, the low dose of Apelin-13 increased anti-inflammatory IL-10 levels more significantly. This effect suggested that low-dose Apelin-13 effectively supported the transition to proliferation in the resolution of the inflammatory phase. The fact that IL-10 levels remained constantly high in Apelin-13 applied groups is because it prevented TGF- β 1 production from reaching pathological levels. Apelin-13 supports IL-10-mediated wound healing in the CCD-1072Sk fibroblast cell line, provides balanced healing, and limits fibrosis formation.

Limitations

This study was conducted on an in vitro scratch wound model using a single human fibroblast cell line (CCD-1072Sk), which may not fully recapitulate the complex cellular and molecular interactions of wound healing in vivo. The lack of a positive control such as epidermal growth factor (EGF) or TGF- β is a limitation of our study. However, our design compensated for this by comparing the control group with the 2 and 5 μ g/ml doses of Apelin-13 and time points. The use of positive controls planned for future in vitro validation studies. This study did not investigate the molecular mechanisms of Apelin-13 in detail; future protein-level analyses (e.g., immunohistochemistry, Western blotting) could provide further insights.

CONCLUSIONS

We investigated the possible effects of Apelin-13 on inflammation, proliferation, migration, and cell survival in the wound model created in the CCD-1072Sk human skin fibroblast cell line. Apelin-13 maintained the proinflammatory and anti-inflammatory balance and facilitated the progression from the inflammatory phase to the proliferation and resolution stages of wound healing. It increased fibroblast cell migration and proliferation, which are necessary for the closure of the wound line, and directed apoptosis in a manner that complies with the physiological wound healing mechanism. 2 μ g-Apelin-13 dose

played a prominent role in showing these effects. However, the 5 µg-Apelin-13 dose was more effective than the low dose at certain time points. Successful wound healing could be achieved if the treatment initiated with high-dose Apelin-13 in the early stages is supported with low-dose Apelin-13 in the later stages, depending on the physiological time points of wound healing. This may be a hypothesis that needs to be tested in future in vivo studies. Further molecular studies are required in this therapeutic strategy.

Acknowledgements: The research was carried out with the valuable support of the Physiology Laboratories at Haliç University-Faculty of Medicine, Istanbul University-Cerrahpaşa, Cerrahpaşa Faculty of Medicine and Istinye University-Faculty of Medicine.

Data Availability: The data that support the findings of this study are available from the corresponding author upon reasonable request.

Funding: This study was supported by the Istanbul University-Cerrahpaşa Scientific Research Projects Coordination Unit (BAP), project no. TSA-2023-37359. The ELISA kits used in this study were purchased under this support.

Conflict of interest: No conflict of interest was declared by the authors.

Informed Consent: Informed consent was not required as no human participants or animal subjects were involved.

Ethical Approval: This study did not require ethical approval since it was performed in vitro using cell lines.

Author Contributions: Conception- K.Y.O., G.A.; Design- K.Y.O., G.A., A.O.; Supervision- H.O.S.; Fundings- H.O.S.; Materials- A.O. K.Y.O., G.A.; Data Collection and/or Processing- K.Y.O., A.O., G.A.; Analysis and/or Interpretation- A.O, K.Y.O.; Literature- K.Y.O., A.O.; Review- K.Y.O., A.O.; Writing- K.Y.O., A.O.; Critical Review- K.Y.O., A.O., G.A.

REFERENCES

- [1] Wilkinson HN, Hardman MJ (2020) Wound healing: Cellular mechanisms and pathological outcomes. *Open Biol.* 10(9):200223. <https://doi.org/10.1098/rsob.200223>
- [2] Peña OA, Martin P (2024) Cellular and molecular mechanisms of skin wound healing. *Nat Rev Mol Cell Biol.* 25(8):599–616. <https://doi.org/10.1038/s41580-024-00715-1>
- [3] Burgess JL, Wyant WA, Abujamra BA, Kirsner RS, Jozic I (2021) Diabetic wound-healing science. *Medicina (Kaunas)* 57(10):1072. <https://doi.org/10.3390/medicina57101072>
- [4] Mayrovitz HN, Wong S, Mancuso C (2023) Venous, arterial, and neuropathic leg ulcers with emphasis on the geriatric population. *Cureus.* 15(4):e38123. <https://doi.org/10.7759/cureus.38123>
- [5] Boyko TV, Longaker MT, Yang GP (2018) Review of the Current Management of Pressure Ulcers. *Adv Wound Care (New Rochelle).* 1;7(2):57-67. <https://doi.org/10.1089/wound.2016.0697>
- [6] Ahmad N (2022) In vitro and in vivo characterization methods for evaluation of modern wound dressings. *Pharmaceutics.* 15(1):42. <https://doi.org/10.3390/pharmaceutics15010042>
- [7] Vang Mouritzen M, Jenssen H (2018) Optimized scratch assay for in vitro testing of cell migration with an automated optical camera. *J Vis Exp.* 138:e57691. <https://doi.org/10.3791/57691>
- [8] Bainbridge P (2013) Wound healing and the role of fibroblasts. *J Wound Care.* 22(8):407–412. <https://doi.org/10.12968/jowc.2013.22.8.407>
- [9] Addis R, Cruciani S, Santaniello S, et al (2020) Fibroblast proliferation and migration in wound healing by phytochemicals: Evidence for a novel synergic outcome. *Int J Med Sci.* 17(8):1030–1042. <https://doi.org/10.7150/ijms.43986>
- [10] Cialdai F, Risaliti C, Monici M (2022) Role of fibroblasts in wound healing and tissue remodeling on Earth and in space. *Front Bioeng Biotechnol.* 10:958381. <https://doi.org/10.3389/fbioe.2022.958381>
- [11] Akhtari N, Ahmadi M, Kiani Doust Vaghe Y, et al (2024) Natural agents as wound-healing promoters. *Inflammopharmacology.* 32(1):101–125. <https://doi.org/10.1007/s10787-023-01318-6>
- [12] Correa-Gallegos D, Jiang D, Rinkevich Y (2021) Fibroblasts

- as confederates of the immune system. *Immunol Rev.* 302(1):147–162. <https://doi.org/10.1111/imr.12972>
- [13] Ina K, Kusugami K, Kawano Y, et al (2005) Intestinal fibroblast-derived IL-10 increases survival of mucosal T cells by inhibiting growth factor deprivation- and Fas-mediated apoptosis. *J Immunol.* 175(3):2000–2009. <https://doi.org/10.4049/jimmunol.175.3.2000>
- [14] Wong R, Tan T, Pang A, Srinivasan D (2025) The role of cytokines in wound healing: From mechanistic insights to therapeutic applications. *Explor Immunol.* 2025;5:1003183. <https://doi.org/10.37349/ei.2025.1003183>
- [15] Shi X, Young D, Zhou H, Wang X (2020) Transforming growth factor- β signaling in fibrotic diseases and cancer-associated fibroblasts. *Biomolecules.* 10(12):1666. <https://doi.org/10.3390/biom10121666>
- [16] Pakyari M, Farrokhi A, Maharlooei K, Ghahary A (2013) Critical role of transforming growth factor beta in different phases of wound healing. *Adv Wound Care (New Rochelle).* 2(5):215–224. <https://doi.org/10.1089/wound.2012.0406>
- [17] Shin K, Kenward C, Rainey K (2017) Apelinergic system structure and function. *Compr Physiol.* 8(1):407–450. <https://doi.org/10.1002/cphy.c170028>
- [18] Park J, Park Y, Kim Y, Jun Y, Lee U, Oh M (2023) Apelin as a new therapeutic target for COVID 19 treatment. *QJM.* 116(3):197–204. <https://doi.org/10.1093/qjmed/hcac229>
- [19] Robillard S, Tr n K, Lachance S, et al (2023) Apelin prevents diabetes induced poor collateral vessel formation and blood flow reperfusion in ischemic limb. *Front Cardiovasc Med.* 10:1191891. <https://doi.org/10.3389/fcvm.2023.1191891>
- [20] Kidoya H, Naito H, Takakura N (2010) Apelin induces enlarged and nonleaky blood vessels for functional recovery from ischemia. *Blood.* 115(15):3166–3174. <https://doi.org/10.1182/blood-2009-07-232306>
- [21] Yamazaki S, Sekiguchi A, Uchiyama A, et al (2020) Apelin/APJ signaling suppresses the pressure ulcer formation in cutaneous ischemia reperfusion injury mouse model. *Sci Rep.* 10(1):1349. <https://doi.org/10.1038/s41598-020-58452-2>
- [22] Shi N, Wang Y, Xia Z, et al (2024) The regulatory role of the apelin/APJ axis in scarring: Identification of upstream and downstream mechanisms. *Biochim Biophys Acta Mol Basis Dis.* 1870(4):167125. <https://doi.org/10.1016/j.bbadis.2024.167125>
- [23] Kari S, Subramanian K, Altomonte A, Murugesan A, Yli Harja O, Kandhavelu M (2022) Programmed cell death detection methods: A systematic review and a categorical comparison. *Apoptosis.* 27(7–8):482–508. <https://doi.org/10.1007/s10495-022-01735-y>
- [24] Malakar D, Dey A, Basu A, Ghosh AK (2008) Antiapoptotic role of S adenosyl L methionine against hydrochloric acid induced cell death in *Saccharomyces cerevisiae*. *Biochim Biophys Acta.* 1780(7–8):937–947. <https://doi.org/10.1016/j.bbagen.2008.03.014>
- [25] Moela P, Motadi LR (2016) RBBP6: A potential biomarker of apoptosis induction in human cervical cancer cell lines. *Oncotargets Ther.* 9:4721–4735. <https://doi.org/10.2147/OTT.S100964>
- [26] Siri wattanasatorn M, Itharat A, Thongdeeying P, Oraikul B (2020) In Vitro Wound Healing Activities of Three Most Commonly Used Thai Medicinal Plants and Their Three Markers. *Evid Based Complement Alternat Med.* 2020:6795383. <https://doi.org/10.1155/2020/6795383>
- [27] Sazonova EV, Chesnokov MS, Zhivotovsky B, Kopeina GS (2022) Drug toxicity assessment: cell proliferation versus cell death. *Cell Death Discov.* 8(1):417. <https://doi.org/10.1038/s41420-022-01207-x>
- [28] Lin T, Zhao Y, Guo S, et al (2022) Apelin 13 protects neurons by attenuating early stage post spinal cord injury apoptosis in vitro. *Brain Sci.* 12(11):1151. <https://doi.org/10.3390/brainsci12111515>
- [29] Samandari-Bahraseman MR, Elyasi L (2021) Apelin-13 protects human neuroblastoma SH-SY5Y cells against amyloid-beta induced neurotoxicity: Involvement of anti oxidant and anti apoptotic properties. *J Basic Clin Physiol Pharmacol.* 33(5):599–605. <https://doi.org/10.1515/jbcpp-2020-0294>
- [30] Martinotti S, Ranzato E (2020) Scratch wound healing assay. In: *Methods Mol Biol.* 2109:225–229. https://doi.org/10.1007/7651_2019_259
- [31] Zhou C, Zhang B, Yang Y, et al (2023) Stem cell derived exosomes: Emerging therapeutic opportunities for wound healing. *Stem Cell Res Ther.* 14(1):107. <https://doi.org/10.1186/s13287-023-03345-0>
- [32] Zhang BH, Guo CX, Wang HX, et al (2014) Cardioprotective

- effects of adipokine apelin on myocardial infarction. *Heart Vessels*. 29(5):679–689. <https://doi.org/10.1007/s00380-013-0425-z>
- [33] Zheng W, Wang J, Xie L, et al (2019) An injectable thermosensitive hydrogel for sustained release of apelin 13 to enhance flap survival in rat random skin flap. *J Mater Sci Mater Med*. 30(9):106. <https://doi.org/10.1007/s10856-019-6306-y>
- [34] Doğan A (2019) Apelin receptor (Aplnr) signaling promotes fibroblast migration. *Tissue Cell*. 56:98–106. <https://doi.org/10.1016/j.tice.2019.01.003>
- [35] Yokoyama Y, Sekiguchi A, Fujiwara C, et al (2018) Inhibitory regulation of skin fibrosis in systemic sclerosis by apelin/APJ signaling. *Arthritis Rheumatol*. 70(10):1661–1672. <https://doi.org/10.1002/art.40533>
- [36] Riwaldt S, Corydon TJ, Pantalone D, et al (2021) Role of apoptosis in wound healing and apoptosis alterations in microgravity. *Front Bioeng Biotechnol*. 9:679650. <https://doi.org/10.3389/fbioe.2021.679650>
- [37] Ishimaru Y, Sumino A, Kajioka D, et al (2017) Apelin protects against NMDA induced retinal neuronal death via an APJ receptor by activating Akt and ERK1/2, and suppressing TNF α expression in mice. *J Pharmacol Sci*. 133(1):34–41. <https://doi.org/10.1016/j.jphs.2016.12.002>
- [38] Li X, Gu C, Hu Q, Wang L, Zhang Y, Yu L (2024) Protective effect of apelin 13 in lens epithelial cells via inhibiting oxidative stress induced apoptosis. *BMC Ophthalmol*. 24(1):479. <https://doi.org/10.1186/s12886-024-03746-6>
- [39] Li S, Yuan S, Yang S, et al (2025) Apelin 13/APJ promotes neural stem cells to repair ischemic stroke. *Tissue Cell*. 95:102872. <https://doi.org/10.1016/j.tice.2025.102872>
- [40] Xu C, Nie X, Xu R, Zhou L, Wang D (2025) Protective effects of apelin 13 on nicotine induced H9c2 cardiomyocyte apoptosis and oxidative stress. *Tob Induc Dis*. 23:201400. <https://doi.org/10.18332/tid/201400>
- [41] Jang DI, Lee AH, Shin HY, et al (2021) The role of tumor necrosis factor alpha (TNF α) in autoimmune disease and current TNF α inhibitors in therapeutics. *Int J Mol Sci* 22(5):2794. <https://doi.org/10.3390/ijms22052719>
- [42] Raziyeveva K, Kim Y, Zharkinbekov Z, Kassymbek K, Jimi S, Saparov A (2021) Immunology of acute and chronic wound healing. *Biomolecules*. 11(5):744. <https://doi.org/10.3390/biom11050700>
- [43] Huang SM, Wu CS, Chiu MH, et al (2019) High glucose environment induces M1 macrophage polarization that impairs keratinocyte migration via TNF- α : An important mechanism to delay the diabetic wound healing. *J Dermatol Sci*. 96(3):159–167. <https://doi.org/10.1016/j.jdermsci.2019.11.004>
- [44] Singampalli KL, Balaji S, Wang X, et al (2020) The role of an IL 10/hyaluronan axis in dermal wound healing. *Front Cell Dev Biol*. 8:636. <https://doi.org/10.3389/fcell.2020.00636>
- [45] Wang J, Xiang H, Lu Y, Wu T (2021) Role and clinical significance of TGF β 1 and TGF β R1 in malignant tumors (Review). *Int J Mol Med*. 47(4). <https://doi.org/10.3892/ijmm.2021.4888>
- [46] Xiaojie W, Banda J, Qi H, et al (2022) Scarless wound healing: Current insights from the perspectives of TGF β , KGF 1, and KGF 2. *Cytokine Growth Factor Rev*. 66:26–37. <https://doi.org/10.1016/j.cytogfr.2022.03.001>
- [47] Peng Y, Wu S, Tang Q, Li S, Peng C (2019) KGF 1 accelerates wound contraction through the TGF β 1/Smad signaling pathway in a double paracrine manner. *J Biol Chem*. 294(21):8361–8370. <https://doi.org/10.1074/jbc.RA118.006189>
- [48] Sziksz E, Pap D, Lippai R, et al (2015) Fibrosis related inflammatory mediators: Role of the IL 10 cytokine family. *Mediators Inflamm*. 2015:764641. <https://doi.org/10.1155/2015/764641>

How to Cite;

Oruc A, Oruc KY, Agturk G, Seymen HO (2025) Wound Healing-Promoting Effects of Apelin-13 in a CCD-1072Sk Fibroblast-Based In Vitro Model. *Eur J Ther*. 31(6):417-428. <https://doi.org/10.58600/eurjther2780>